HHS Public Access

Author manuscript

Nature. Author manuscript; available in PMC 2016 August 10.

Published in final edited form as:

Nature. 2016 March 3; 531(7592): 105–109. doi:10.1038/nature16951.

DERIVING HUMAN ENS LINEAGES FOR CELL THERAPY AND DRUG DISCOVERY IN HIRSCHSPRUNG'S DISEASE

Faranak Fattahi[1,2,4], **Julius A Steinbeck**[1,2], **Sonja Kriks**[1,2], **Jason Tchieu**[1,2], **Bastian Zimmer**[1,2], **Sarah Kishinevsky**[1,2,4], **Nadja Zeltner**[1,2], **Yvonne Mica**[1,2,+], **Wael El-Nachef**[5], **Huiyong Zhao**[3], **Elisa de Stanchina**[3], **Michael D. Gershon**[6], **Tracy C. Grikscheit**[5], **Shuibing Chen**[7], and **Lorenz Studer**[1,2]

[1]The Center for Stem Cell Biology, New York, NY 10065

[2]Developmental Biology Program, Sloan-Kettering Institute for Cancer Research, New York, NY 10065

[3]Molecular Pharmacology Program, New York, NY 10065

[4]Weill Graduate School of Medical Sciences of Cornell University, New York, NY 10065.

[5]Children's Hospital Los Angeles, Pediatric Surgery , Los Angeles, CA, United States, 90027

[6]Department of Pathology and Cell Biology, Columbia University, College of Physicians and Surgeons, New York, NY, 10032

[7]Department of Surgery, Weill Medical College of Cornell University, New York, NY 10065.

Abstract

The enteric nervous system (ENS) is the largest component of the autonomic nervous system with neuron numbers surpassing those present in the spinal cord[1]. The ENS has been called the "second brain"[1] given its autonomy, remarkable neurotransmitter diversity and complex cytoarchitecture. Defects in ENS development are responsible for many human disorders including Hirschsprung's disease (HSCR). HSCR is a caused by the developmental failure of ENS progenitors to migrate into the GI tract in particular the distal colon[2]. Human ENS development remains poorly understood due to the lack of an easily accessible model system.

Correspondence: Dr. Lorenz Studer, The Center for Stem Cell Biology, Developmental Biology Program, Memorial Sloan-Kettering Cancer Center, 1275 York Ave, Box 256, New York, NY 10065, Phone 212-639-6126, FAX: 212-717-3642, ; Email: studerl@mskcc.org

[+]Current address: Thermo Fisher Scientific

AUTHOR CONTRIBUTIONS

F.F.: Design and conception of the study, writing of manuscript, maintenance, directed differentiation and gene targeting of human PSCs, establishing of co-culture assays, cellular/molecular assays, histological analyses, small molecule screen. J.A.S.: Establishing optogenetic hESC line and *in vitro* connectivity assays. S.K.: Design and execution of chick transplantation assays. J.T.: RNAseq experimental design and data analysis, B.Z.: Design and data quantification for use of scratch assay. S.K. Biochemical analysis of EDNRB$^{-/-}$ cells. N.Z.: Design of scratch assay. Y.M.: Chick transplantation of melanocyte competent NC. W.E.-N.: Tissue-engineered intestine assay. E.dS.: Design and execution of colon injection assays in NSG and EDNRB mutant mice. H. Z.: Colon injection assays in NSG and EDNRB mutant mice. M.G.: Study design and data interpretation. T.G.: Design and execution of tissue-engineered intestine assays. S.C.: Design and interpretation of small molecule screen and follow up experiment. L.S.: Design and conception of the study, data interpretation, writing of manuscript.

Here we demonstrate the efficient derivation and isolation of ENS progenitors from human pluripotent stem cells (hPSCs) and their further differentiation into functional enteric neurons. *In vitro* derived ENS precursors are capable of targeted migration in the developing chick embryo and extensive colonization of the adult mouse colon. In vivo engraftment and migration of hPSC-derived ENS precursors rescues disease-related mortality in HSCR mice (EDNRB$^{s\text{-}l/s\text{-}l}$), though mechanism of action remains unclear. Finally, EDNRB null mutant ENS precursors enable modeling of HSCR-related migration defects and the identification of Pepstatin A as candidate therapeutics. Our study establishes the first hPSC-based platform for the study of human ENS development and presents cell and drug-based strategies for the treatment of HSCR.

The in vitro derivation of human ENS lineages from hPSCs has remained elusive despite the great medical needs. The ENS develops from both the vagal and sacral NC. We focused on the vagal NC that generates the majority of the ENS and migrates caudally to colonize the entire length of the bowel[2]. Current NC differentiation protocols[3] result in SOX10+ NC precursors that are HOX negative (indicative of anterior/cranial identity; cranial NC (CNCs)). In contrast, vagal NC identity is characterized by the expression of specific, regionally restricted HOX genes including HOXB3[4] and HOXB5[5]. Retinoic acid (RA) has been used previously as an extrinsic factor to shift the regional identity of CNS precursors from anterior to more caudal fates during motoneuron specification[6]. Here we tested whether the addition of RA can similarly direct the regional identity in NC lineages and induce the expression of vagal markers (**Fig. 1a**). Upon RA exposure we obtained *Sox10::GFP*+ NC precursors with yields comparable to CNC conditions, indicating that RA treatment does not interfere with overall NC induction (**Fig. 1b; Extended Data Fig. 1a,b**). To facilitate the isolation of pure NC populations we performed a candidate surface marker screen and identified CD49D (α4-integrin) as an epitope that reliably marks early SOX10+ NC lineages (**Fig. 1b, Extended Data Fig. 1a-c**). We next used CD49D to demonstrate robustness of RA-based NC induction across hPSC lines (both human embryonic (hESCs) and induced pluripotent (hiPSCs) stem cells; **Extended Data Fig. 1d**). Purified CD49D+ NC precursors, derived in the presence of RA, expressed *HOXB2-B5* indicative of vagal identity[4,5] but not more caudal HOX transcripts such as *HOXB9* (**Fig. 1c**). In further agreement with vagal identity, CD49D+, RA-treated NC precursors expressed markers of early enteric NC (ENC) lineages[2] including PAX3, EDNRB and RET (**Fig. 1d, Extended Data Fig. 1e,f**). Given the paucity of developmental data on human ENC development we performed RNAseq analysis in hESC-derived ENC precursors, in cranial NC (CNC) (no RA), in melanocyte-biased NC (MNC) (**Extended Data Fig. 1a**) and in stage-matched CNS precursors[7]. Unsupervised clustering reliably segregated the transcriptomes of all hPSC-derived NC populations away from CNS precursors and further subdivided the various NC sublineages (**Fig. 1e**). The most differentially expressed genes in the ENC compared to CNS lineage included general NC markers such as *FOXD3* or *TFAP2A* but also *PAX3* and *HOX* genes related to the ENC lineage (**Fig. 1f**). CNC and MNC were also enriched in general NC markers but showed high levels of *NEUROG1, ISL1* or *MLANA, TYR, DCT* expression respectively, compatible with their subtype identity (**Extended Data Fig. 1g,h**). Direct comparison of the various NC lineages yielded novel candidate marker of human vagal NC/ENC lineage (**Fig. 1f**). A list of the top 200 enriched transcripts for each NC lineage is

provided (**Supplementary Tables 1-3**). RNAseq data are available at GEO http://www.ncbi.nlm.nih.gov/geo/ accession#: GSE66148.

One key functional property of the ENC is the ability to migrate extensively and to colonize the gut[2]. RFP-labeled, CD49D+ purified (**Fig. 1g**) hPSC-derived ENC precursors were injected into the developing chick embryo at the level of the vagal NC. Transplanted human cells migrated along the trunk of the embryo (**Fig. 1h**) and colonized the gut (22 embryos of 57 injected; **Fig. 1i**). In contrast, stage-matched CNC or MNC precursor targeted cranial regions (CNC) or followed a trajectory along the dermis (MNC) (**Extended Data Fig. 1i**).

To address whether hESC-derived ENC precursors are capable of recreating ENS neuronal diversity we maintained purified CD49D+ ENC precursors in 3D spheroids for 4 days followed by differentiation as adherent cultures in the presence of ascorbic acid and GDNF (**Fig. 2a**). The 3D spheroid step was required to retain high levels of *SOX10::GFP* expression (**Fig. 2b**). Replating of 3D spheroids under differentiation conditions yielded immature neurons expressing Tuj1 and the enteric precursor marker PHOX2A (day 20; **Fig. 2b**). The majority of PHOX2A+ cells were positive for TRKC (NTRK3), a surface marker expressed in enteric neuron precursors[8] suitable for enrichment for PHOX2A+ and ASCL1+ precursors (**Extended Data Fig. 2a,b**). Temporal expression analyses (**Extended Data Fig. 2c-e**) showed maintenance of ENC neuronal precursor marker expression by day 40 of differentiation (**Fig. 2c,d**) followed by an increase in the percentage of mature neurons by day 60 (**Fig. 2e,f**). In agreement with enteric neuron identity we observed a broad range of neurotransmitter phenotypes including 5HT+, GABA+ and NOS+ neurons. The presence of these neurotransmitters in neurons derived from CD49D+ purified NC precursors indicates ENC origin, since those neurotransmitters are not expressed in other NC lineages. Indeed, no 5HT+ neurons were observed in parallel cultures derived from HOX-negative, CD49D+ cells (**Extended Data Fig. 3a,b**). CNC-derived precursors differentiated into tyrosine hydroxylase (TH) expressing neurons (**Extended Data Fig. 3c**) and gave rise to TRKB-(NTRK2) rather than TRKC-positive precursors suggesting enrichment for sympathetic neuron lineages (**Extended Data Fig. 3d,e**).

A major function of the ENS is the control of peristaltic gut movements. We probed the functionality of *in vitro* derived enteric neurons by assessing connectivity with smooth muscle cells (SMCs). hESC-derived SMCs were generated via a mesoderm intermediate following exposure to activin A and BMP4 *in vitro*[9] and culture in the presence of TGFβ (**Extended Data Fig. 4a**). The resulting SMC progenitors expressed ISL1 and were immunoreactive for smooth muscle actin (SMA) (**Extended Data Fig. 4b**). For connectivity studies, enteric neurons were derived from a hESC line expressing channelrhodopsin-2 (ChR2)-EYFP under control of the human Synapsin promoter. An optogenetic reporter line[10] was used to allow for light-induced control of neuronal activity (**Fig. 2g**). GABA+ and 5HT+ neurons in these co-cultures were closely associated with SMCs (**Extended Data Fig. 4c**). Interestingly, co-culture of day 25 neurons with SMCs triggered accelerated neuronal maturation as illustrated by the increased expression of *SYN::EYFP* (**Extended Data Fig. 4d**). Conversely, hESC-derived SMCs also showed signs of accelerated maturation under co-culture conditions as illustrated by the expression of mature markers (MYH11, AchR;

Extended Data Fig. 4e) and the ability to contract in response to pharmacological stimulation (,**Supplementary videos 1-6, Extended Data Fig. 4f**). While no spontaneous contractions were observed under co-culture conditions, a wave of SMC contractions could be triggered 5-10 seconds following light-mediated activation (10 Hz frequency) of *SYN::ChR2-EYFP* neurons (**Fig. 2h,i; Supplementary video 7**). Interestingly, both light- and drug-induced SMC contractions were slow and involved the movement of sheet-like structures suggesting coordination among cells possibly via gap junction-mediated coupling. These studies demonstrate functional connectivity between hESC-derived enteric neurons and SMCs. *In vivo* interactions of the ENS within the gut, however, are more complex and involve multiple cell types. As a first step in modeling those interactions in 3D, we used a tissue engineering approach combining *in vitro* derived human ENC precursors (CD49D+; day 15) with murine primary intestinal tissue (**Extended Data Fig. 5a**). Using our previously established protocols to form organoid units[11], the recombined tissue constructs were seeded onto a scaffold and implanted onto the omentum of immunodeficient hosts for maturation *in vivo*[11]. Human cells were readily detected within gut-like structures using the human-specific SC121 and synaptophysin. Importantly, cells were located both in epithelial and muscle layers (**Extended Data Fig. 5b**), showing their ability to interact with both target cell types.

Transplantation of hPSC-derived precursors could yield novel therapeutic opportunities for ENS disorders such as HSCR. Children suffering from HSCR are currently treated by surgical removal of the aganglionic portion of the gut. While life-saving, the surgery does not address dysfunction of the remaining GI tract in surviving patients[12]. Furthermore, therapeutic options in patients with total aganglionosis are limited. A major challenge in developing a cell therapy for HSCR is the need to repopulate the ENS over extensive distances. Previous studies tested the transplantation of variety of candidate cell sources into the fetal or postnatal colon[13,14]. Murine, fetal-derived ENC precursors resulted in the most promising data with evidence of functional integration but limited *in vivo* migration[15]. To assess the ability of hESC-derived enteric NC precursors to migrate within the postnatal or adult colon (3-6 weeks of age), we performed orthotopic (OT) injections of CD49D+ RFP-labeled precursors in NOD-*scid* IL2Rgamma^{null} (NSG) mice (**Fig. 3a**). Cells were injected into the wall of the cecum aiming for the muscle layer (**Fig. 3a**) and resulting in a well-defined deposit of RFP+ cells 1 hour after injection (**Extended Data Fig. 6a**; left panel; **Fig. 3b**; top panel). Remarkably, 2 – 4 weeks after transplantation, RFP+ cells had migrated extensively and repopulated the host colon over its entire length (**Fig. 3b**). The grafted ENC precursors formed clusters along the colon (**Extended Data Fig. 6a**; right panel) expressing TUJ1 (**Fig. 3c**). In contrast, stage-matched CNS and CNC precursors, grafted under identical conditions, showed limited migration (**Extended Data Fig. 6b,c**).

Given the extraordinary ability of the grafted cells to repopulate the host colon, we tested whether those cells could provide therapeutic benefit in an HSCR model. One widely used genetic model is the EDNRB $^{s\text{-}l/s\text{-}l}$ mouse[16]. These mice develop a megacolon due to aberrant peristalsis. As a consequence, mutant mice show high mortality by 4-6 weeks of age. EDNRB $^{s\text{-}l/s\text{-}l}$ mice were injected at 2-3 weeks after birth with RFP+ hESC-derived enteric NC precursors (treatment group) or with matrigel vehicle (control group). The

majority of control-injected animals (n = 6) died over a period of 4-5 weeks (**Fig. 3d**) with a megacolon-like pathology (**Extended Data Fig. 6d**). In contrast, all animals injected with hESC-derived NC precursors (n=6) survived (**Fig. 3d**). Grafted animals were assessed for graft survival and migration at 6-8 weeks of age. Whole mount fluorescence imaging confirmed migration of hESC-derived ENC precursors within the HSCR colon (**Extended Data Fig. 6 e,f**). Preliminary studies showed a trend towards an improved GI transit time in grafted versus the small subset of matrigel treated animals that survived beyond 6 weeks of treatment, as measured using carmine dye gavage (**Extended Data Fig. 6g**). Histological analyses at 6 weeks and 3 months after transplantation confirmed myenteric and submucosal localization of human cells in HSCR colon. While the location mimicked aspects of endogenous ENS, there was a preference towards submucosal region (**Fig. 3e; Extended Data Fig. 6h**, upper panel). Human cells were also detected in the distal colon (**Extended Data Fig. 6h**, lower panel) where only few endogenous TUJ1+ cells were detected. Immunocytochemistry for SC121 and human-specific synaptophysin, not detected in matrigel injected animals (**Extended Data Fig. 6i**), confirmed human identity and pre-synaptic marker expression (**Fig. 3f**, right panel). In addition to neuronal cells (**Extended Data Fig. 6h**) we also observed human cells expressing glial marker including GFAP (**Extended Data Fig. 6j**). Neuron subtype specific markers in SC121+ human cells included 5-HT, GABA and NOS (**Fig. 3f; Extended Data Fig. 6k,l**).

Our findings demonstrate that wild-type hPSC-derived ENS precursors can repopulate the colon of HSCR mice. However, HSCR-causing mutations often affect the migration of ENS precursor in a cell autonomous manner[2,17]. Therefore, developing patient-matched cell therapies for HSCR may require complementary genetic or pharmacological strategies to overcome intrinsic migration defects of the transplanted cells. As causative genetic defects in HSCR patients are often not known or complex[2,18] gene correction prior to transplantation may not be possible. We therefore assessed whether hPSC-derived ENS precursors can be used to model HSCR and serve as a platform to screen for candidate compounds that could overcome disease-related migration defects. In a first step we established isogenic hESC lines with homozygous loss-of-function mutations in EDNRB using CRISPR/Cas-based gene targeting techniques[19] (**Fig. 4a, Extended Data Fig. 7a,b**). Loss of function mutations in EDNRB are a well-known genetic cause in a subset of HSCR patients[20]. Enteric NC precursors could be derived at comparable efficiencies from EDNRB-mutant and control lines (**Extended Data Fig. 7c**). However, CD49D+ ENC precursors from four EDNRB $^{-/-}$ clones showed a striking migration defect when using the scratch assay to model aspects of HSCR phenotype[21] (**Fig. 4b,c**). We next assessed whether EDNRB–/– ENCs display major differences in cell proliferation or survival as compared to wild-type ENCs. At 24 hours after replating (time point used for scratch assay) we did not observe differences in either assay (**Extended Data Fig. 7d,e**). By 72 hours, EDNRB–/– ENCs did show reduced proliferation while cell viability remained unaffected (**Extended Data Fig. 7d,e**).

We next carried out a small molecule screen to identify compounds capable of rescuing the migration defects observed in EDNRB mutant ENC precursors (**Fig. 4d; Extended Data Fig. 8a**). We screened 1280 compounds (Prestwick Chemical Library®) comprised of FDA-

approved drugs. Results were binned into compounds with no effect, toxic effects, modest effects or strong effects (**Fig. 4d, Extended Data Fig. 8a-c**). The hits were further validated by repeating scratch assay under non-HTS conditions (**Extended Data Fig. 8d**). Compounds with strong effects were chosen for further follow-up. Among those validated compounds we focused on the molecule Pepstatin A which showed a dose-dependent rescue of the migration defect in EDNRB$^{-/-}$ hESC derived NC precursors (**Fig. 4e**). Pepstatin A is a known inhibitor of acid proteases[22]. Among potential Pepstatin targets we explored BACE2 because RNAseq data showed upregulation in hESC-derived NC lineages (**Extended Data Fig. 9a**) and BACE-2 had been recently shown to modulate migration of NC derivatives in the developing zebrafish embryo[23]. To address whether BACE2 mediates the Pepstatin A effect, we tested structurally unrelated small molecules targeting BACE2. Exposure to the BACE inhibitor IV rescued migration defect in the scratch assay similar to Pepstatin A (**Fig. 4f**). Furthermore, BACE2 knockdown confirmed rescue of the migration defect in EDNRB$^{-/-}$ cells (**Extended Data Fig. 9b; Fig. 4g**). Finally, we tested whether Pepstatin A exposure *in vitro* is sufficient to rescue the *in vivo* migration behavior of EDNRB$^{-/-}$ ENC precursors (**Fig. 4h**). ENC precursors derived from EDNRB$^{-/-}$ cells exhibit a significant *in vivo* migration defect following transplantation into the adult colon (**Fig. 4i,j**). EDNRB-null precursors pre-treated with Pepstatin A for 72 hours before transplantation showed a significant rescue of *in vivo* migration (**Fig. 4i,j; Extended Data Fig. 9c**). Interestingly, wild-type derived ENC precursors treated with pharmacological inhibitors of EDNRB showed migration defects *in vitro* and *in vivo* (**Extended Data Fig. 9d-f**) further supporting a role for EDNRB in human ENC migration and HSCR.

Our study describes an efficient strategy to derive and prospectively purify ENC precursors from hESCs. In agreement with studies in model organisms[1,2] we demonstrate that hESC-derived ENC gives rise to a broad range of neurotransmitter phenotypes characteristic of the ENS. The ability to model human ENS development *in vitro* should enable the large-scale production of specific human enteric neurons on demand. For example hPSC-derived enteric 5HT-neurons could serve as a tool to model GI side effects of CNS-acting drugs such as Prozac[1].

We focused primarily on potential cell therapeutic applications of hESC-derived ENC lineages in HSCR. One of the most remarkable findings was the extensive *in vivo* migratory potential of human ENC precursors in the adult host colon. Future studies will have to define whether this ability is confined to early CD49D+ cells or maintained at later neurogenic stages. Similarly, it will be important to look at long-term efficacy and safety. While most of our *in vivo* studies in NSG mice (a total of 102 animals grafted) were limited to a 5-6 week survival period, animals analyzed at 3-4 months after transplantation showed comparable *in vivo* properties without evidence of tumor formation or graft-related adverse effects. The therapeutic potential of the cells is illustrated by their ability to rescue EDNRB$^{s-l/s-l}$ mice. Future studies will be required to address mechanisms of the graft-mediated host rescue. The potential for widespread engraftment may eventually enable permanent, bona fide repair of the aganglionic portions of the gut. However, given the rapid action of the cells in preventing death of HSCR mice, it appears unlikely that rescue was mediated by functional integration of the cells. Future studies should also address alternative mechanisms such as cytokine

release, immunomodulation or changes in barrier function for contributing to the therapeutic effect.

The identification of Pepstatin A and BACE2 inhibition in rescuing HSCR-related migration defects represents proof-of-concept for the use of hESC-derived ENC precursors in drug discovery. The mechanism of BACE-2 inhibition on migration remains to be elucidated. Possible targets of BACE proteases include neuregulins and ErbB receptors previously implicated in NC migration[24,25]. One obvious future direction is testing the therapeutic potential of BACE inhibitors in mouse models of HSCR. Such a strategy could enable the prevention of aganglionosis during pregnancy or enable repair of postnatal enteric neuron function. In the current study we focused on combining Pepstatin A as a neoadjuvant treatment to promote migration of EDNRB$^{-/-}$ enteric NC precursors. An important next question is whether Pepstatin A-pretreated cells are capable of rescuing lethality or other disease-associated phenotypes in HSCR mice. In conclusion, our work presents a powerful strategy to access human ENS lineages for exploring the "second brain[1]" in human health and disease and for developing novel cell- and drug-based therapies for HSCR.

MATERIALS & METHODS

Culture of undifferentiated human Embryonic Stem cells (hESCs)

hESC line H9 (WA-09) and derivatives (SOX10::GFP; SYN::ChR2-EYFP; SYN::EYFP;PHOX2B:GFP ;EF1::RFP EDNRB−/−) as well as 2 independent hiPSC lines (healthy and Familial Dysautonomia, Sendai-based, OMSK (Cytotune)) were maintained on mouse embryonic fibroblasts (MEF, Global Stem, Rockville, MD) in KSR (Life Technologies, 10828-028) containing hESC medium as described previously[7]. Cells were subjected to mycoplasma testing at monthly intervals and STR profiled to confirm cell identity at the initiation of the study.

Neural Crest induction

hESCs were plated on matrigel (BD Biosciences, 354234) coated dishes (10^5 cells/cm^2) in hESC medium containing 10nM FGF2 (R&D Systems, 233-FB-001MG/CF). Differentiation was initiated in knockout serum replacement (KSR) medium (KO DMEM+15% KSR (Life Technologies, 10828-028), L-glutamine (Life Technologies, 25030-081), NEAA (Life Technologies, 11140-050) containing LDN193189 (100nM, Stemgent, Cambridge, MA) and SB431542 (10μM, Tocris, Ellisville, MI). The KSR medium was gradually replaced with increasing amounts of N2 medium from day 4 through day 10 as described previously[7]. For Cranial NC (CNC) induction, cells are treated with 3μM CHIR99021 (Tocris Bioscience, 4423) in addition to LDN193189 and SB431542 from day 2 through day 11. Enteric NC (ENC) differentiation involves additional treatment with Retinoic Acid (10μM) from day 6 through day11. For deriving Melanocyte-competent NC (MNC), LDN193189 is replaced with BMP4 (10nM, R&D, 314-bp) and EDN3 (10nM, American Peptide company, 88-5-10B) from day 6 through day 11[3]. The differentiated cells are sorted for CD49D at day 11. CNS precursor control cells were generated by treatment with LDN193189 and SB431542 from day 0 through day 11 as previously described[7]. Throughout the manuscript, day 0 is the day the medium is switched from hESC medium to LDN193189 and SB431542

containing medium. Days of differentiation in text and figures refer to the number of days since the pluripotent stage (day 0).

FACS and Immunofluorescence analysis (IF)

For IF, the cells were fixed with 4% paraformaldehyde (PFA) (Affymetrix-USB, 19943) for 20 minutes, then blocked and permeabilized using 1% Bovine Serum Albumin (BSA) (Thermo Scientific, 23209) and 0.3% triton X-100 (Sigma, T8787). The cells were then incubated in primary antibody solutions overnight at 4°C (Celsius) and stained with fluorophore conjugated secondary antibodies at RT for 1 hour The stained cells were then incubated with DAPI (1 ng/ml, Sigma, D9542-5MG) and washed several times before imaging. For Flow Cytometry analysis, the cells are dissociated with Accutase (Innovative Cell Technologies, AT104) and fixed and permeabilized using BD Cytofix/Cytoperm (BD Bioscience, 554722) solution, then washed, blocked and permeabilized using BD Perm/Wash buffer (BD Bioscience, 554723) according to manufacturer's instructions. The cells are then stained with primary (overnight at 4°C) and secondary (30 min at room temperature) antibodies and analyzed using a flow Cytometer (Flowjo software). A list of primary antibodies and working dilutions is provided in Supplementary **Table 4**. The PHOX2A antibody was kindly contributed by Dr. J-F Brunet (Rabbit, 1:800 dilution).

In ovo transplants

Fertilized eggs (from Charles River farms) were incubated at 37°C for 50 hours before injections. 2×10^5 CD49D sorted, RFP labeled NC cells were injected into the intersomitic space of the vagal region of the embryos targeting a region between somite 2 and 6 (HH 14 embryo, 20-25 somite stage). The embryos were harvested 36 hours later for whole mount epifluorescence and histological analyses.

Gene expression analysis

For RNA sequencing, total RNA was extracted using RNeasy RNA purification kit (Qiagen, 74106). For qRT-PCR assay, total RNA samples were reverse transcribed to cDNA using Superscript II Reverse Transcriptase (Life Technologies, 18064-014). qRT-PCR reactions were set up using QuantiTect SYBR Green PCR mix (Qiagen, 204148). Each data point represents three independent biological replicates.

In vitro differentiation of ENC to enteric neurons

ENC cells from the 11 day induction protocol were aggregated into 3D spheroids (5 million cells/well) in Ultra Low Attachment 6-well culture plates (Fisher Scientific, 3471) and cultured in Neurobasal (NB) medium supplemented with L-Glutamine (Gibco, 25030-164), N2 (Stem Cell Technologies, 07156) and B27 (Life Technologies, 17504044) containing CHIR99021 (3uM, Tocris Bioscience, 4423) and FGF2 (10nM, R&D Systems, 233-FB-001MG/CF). After 4 days of suspension culture, the spheroids are plated on Poly Ornithine/Laminin/Fibronectin (PO/LM/FN) coated dishes (prepared as described previously[26]) in Neurobasal (NB) medium supplemented with L-Glutamine (Gibco, 25030-164), N2 (Stem Cell Technologies, 07156) and B27 (Life Technologies, 17504044) containing GDNF (25 ng/ml, Peprotech, 450-10) and Ascorbic acid (100 uM, Sigma,

A8960-5G). The ENC precursors migrate out of the plated spheroids and differentiate into neurons in 1-2 weeks. The cells were fixed for immunostaining or harvested for gene expression analysis at Day 25, Day 40 and Day 60 of differentiation.

Induction of SMCs

Mesoderm specification is carried out in STEMPRO-34 (Gibco, 10639-011) medium. The hESCs are subjected to Activin A treatment (100ng/ml, R&D, 338-AC-010) for 24 hours followed by BMP4 treatment (10ng/ml, R&D, 314-bp) for four days[9]. The Cells are then differentiated into SMC progenitors by treatment with PDGF-BB (5 ng/ml, Peprotech, 100-14B) , TGFb3 (5 ng/ml, R&D systems, 243-B3-200) and 10% FBS. The SMC progenitors are expandable in DMEM supplemented with 10% FBS.

EN-SMC co-culture

The SMC progenitors were plated on PO/LM/FN coated culture dishes (prepared as described previously[26]) three days before addition of ENC-derived neurons. The neurons were dissociated (using accutase, Innovative Cell Technologies, AT104) at day 30 of differentiation and plated onto the SMC monolayer cultures. The culture is maintained in Neurobasal (NB) medium supplemented with L-Glutamine (Gibco, 25030-164), N2 (Stem Cell Technologies, 07156) and B27 (Life Technologies, 17504044) containing GDNF (25 ng/ml, Peprotech, 450-10) and Ascorbic acid (100 uM, Sigma, A8960-5G). Functional connectivity was assessed at 8-16 weeks of co-culture.

Pharmacological and optogenetic stimulations of co-cultured SMCs

SMC only and SMC-ENC-derived neuron co-cultures were subjected to Acetylcholine chloride (50μM, Sigma, A6625), Carbamoylcholine chloride (10μM, Sigma,C4382) and KCl (55mM) Fisher scientific, BP366-500) treatment, 3 months after initiating the co-culture. Optogenetic stimulations were performed using a 450 nm pigtailed diode pumped solid state laser (OEM Laser, PSU-III LED, OEM Laser Systems, Inc) achieving an illumination between 2 and 4 mW/mm^2. The pulse width was 4 ms and stimulation frequencies ranged from 2 to 10 Hz. For the quantification of movement, images were assembled into a stack using Metamorph software and regions with high contrast were identified (labeled yellow in fig. S5). The movement of 5 representative high contrast regions per field was automatically traced (Metamorph software). Data is presented in kinetograms as movement in pixels in x and y direction (distance) with respect to the previous frame.

Generation of chimeric tissue engineered colon (TEC)

We used the previously described method for generation of TEC [11]. Briefly, the donor colon tissue was harvested and digested into organoid units using dispase (Life Technologies, 17105-041) and collagenase type 1 (Worthington, CLS-1). The organoid units were then mixed immediately (without any *in vitro* culture) with CD49D purified hESC-derived ENC precursors (day 15 of differentiation) and seeded onto biodegradable Polyglycolic Acid Scaffolds (2-mm sheet thickness, 60 mg cm-3 bulk density; porosity > 95%, Concordia Fibers, Coventry RI) shaped into 2mm long tubes with Poly- L Lactide (PLLA) (Durect Corporation). The seeded scaffolds were then placed onto and wrapped in the greater

omentum of the adult (>2 months old) NSG mice. Just prior to the implantation, these mice were irradiated with 350 cGY. The seeded scaffolds were differentiated into colon-like structures inside the omentum for 4 additional weeks before they were surgically removed for tissue analysis.

Transplantation of ENC precursors in adult colon

All mouse procedures were performed following NIH guidelines, and were approved by the local Institutional Animal Care and Use Committee (IACUC), the Institutional Biosafety Committee (IBC) as well as the Embryonic Stem Cell Research Committee (ESCRO). 3-6 week old male NSG (NOD.Cg-*Prkdc*^{scid} *Il2rg*^{tm1Wjl}/SzJ) mice or 2-3 weeks old EDNRB$^{s\text{-}l/s\text{-}l}$ (SSL/LeJ) mice[27] (n=12, 6 male, 6 female) were used for these studies. Animal numbers were based on availability of homozygous hosts and on sufficient statistical power to detect large effects between treatment versus control (EDNRB$^{s\text{-}l/s\text{-}l}$) as well as for demonstrating robustness of migration behavior (NSG). Animals were randomly selected for the various treatment paradigms (NSG and EDNRB $^{s\text{-}l/s\text{-}l}$) but assuring for equal distribution of male/female ratio in each group (EDNRB $^{s\text{-}l/s\text{-}l}$). Animals were anesthetized with isoflurane (1%) throughout the procedure, a small abdominal incision was made, abdominal wall musculature lifted and the cecum is exposed and exteriorized. Warm saline is used to keep the cecum moist. 20 μl of cell suspension (2-4 million RFP+ CD49D purified hESC-derived ENC precursors) in 70% matrigel (BD Biosciences, 354234) in PBS or 20 μl of 70% matrigel in PBS only (control grafted animals) were slowly injected into the cecum (targeting the muscle layer) using a 27-gauge needle. Use of 70% matrigel as carrier for cell injection assured that the cells stayed in place following the injection and prevented backflow into peritoneum. After injection that needle was withdrawn, and a Q-tip was placed over the injection site for 30 seconds to prevent bleeding. The cecum was returned to the abdominal cavity and the abdominal wall was closed using 4-0 vicryl and a taper needle in an interrupted suture pattern and the skin was closed using sterile wound clips. After wound closure animals were put on paper on top of their bedding and attended until conscious and preferably eating and drinking. The tissue was harvested at different time points (ranging from two weeks to four months) after transplantation for histological analysis. EDNRB$^{s\text{-}l/s\text{-}l}$ mice were immunosuppressed by daily injections of cyclosporine (10mg/kg i.p, Sigma, 30024).

Whole mount fluorescence imaging and histology

The harvested colon samples were fixed in 4% PFA at 4°C overnight before imaging. Imaging is performed using Maestro fluorescence imaging system (Cambridge Research and Instrumentation). The tissue samples were incubated in 30% sucrose (Fisher Scientific, BP220-1) solutions at 4°C for 2 days then embedded in OCT (Fisher Scientific, NC9638938) and cryosectioned. The sections were then blocked with 1% BSA (Thermo Scientific, 23209) and permeabilized with 0.3% Triton X-100 (Sigma, T8787). The sections are then stained with primary antibody solution at 4°C overnight and fluorophore conjugated secondary antibody solutions at room temperature for 30 minutes. The stained sectioned were then incubated with DAPI (1 ng/ml, Sigma, D9542-5MG) and washed several times before they were mounted with Vectashield Mounting Medium (vector, H1200) and imaged using fluorescent (Olympus IX70) or confocal microscopes (Zeiss SP5).

Total GI transit time

Mice are gavaged with 0.3 ml of dye solution containing 6% carmine (Sigma, C1022-5G), 0.5% methylcellulose (Sigma, 274429-5G) and 0.9 NaCl, using a #24 round-tip feeding needle. The needle was held inside the mouse esophagus for a few seconds after gavage to prevent regurgitation. 1 hour later, the stool color was monitored for gavaged mice every 10 minutes. For each mouse, total GI transit time is between the time of gavage and the time when red stool is observed.

Gene targeting

The double nickase CRISPR/Cas9 system[28] was used to target the EDNRB locus in *EF1::RFP* H9 hESCs. Two guide RNAs were designed (using the CRISPR design tool http://crispr.mit.edu/) to target the coding sequence with PAM targets ~20 bp apart (qRNA #1 target specific sequence: AAGTCTGTGCGGACGCGCCCTGG, RNA #2 target specific sequence: CCAGATCCGCGACAGGCCGCAGG). The cells were transfected with gRNA constructs and GFP-fused Cas9-D10A nickase. The GFP expressing cells were FACS purified 24 hours later and plated in low density (150 cells/cm^2) on MEFs. The colonies were picked 7 days later and passaged twice before genomic DNA isolation and screening. The targeted region of EDNRB gene was PCR amplified (forward primer: ACGCCTTCTGGAGCAGGTAG, reverse primer: GTCAGGCGGGAAGCCTCTCT) and cloned into Zero Blunt TOPO vector (Invitrogen, 450245). To ensure that both alleles (from each hESC colony) are represented and sequenced, we picked 10 bacterial clones (for each hESC clone) for plasmid purification and subsequent sequencing. The clones with bi-allelic nonsense mutations were expanded and differentiated for follow-up assays.

Migration assay

The ENC cells are plated on PO/LM/FN coated (prepared as described previously[26]) 96well or 48well culture plates (30,000/cm^2). 24 hours later the culture lawn is scratched manually using a pipette tip. The cells are given an additional 24-48 hours to migrate into the scratch area and fixed for imaging and quantification. The quantification is based on the percentage of the nuclei that are located in the scratch area after the migration period. The scratch area is defined using a reference well that was fixed immediately after scratching. Migration of cells was quantified using the open source data analysis software KNIME[29] (http://knime.org) with the "Quantification in ROI" plug-in as described in detail elsewhere[30].

Proliferation assay

To quantify proliferation, FACS purified ENC cells were assayed using CyQUANT NF cell proliferation Assay Kit (Life Technologies, C35006) according to manufacturer's instructions. Briefly, to generate a standard, cells were plated at various densities and stained using the fluorescent DNA binding dye reagent. Total fluorescence intensity was then measured using a plate reader (excitation at 485 nm and emission detection at 530 nm). After determining the linear range, the CD49D+ WT and EDNRB$^{-/-}$ ENC precursors were plated (6000 cell/cm^2) and assayed at 0, 24, 48 and 72 hrs. The cells were cultured in Neurobasal (NB) medium supplemented with L-Glutamine (Gibco, 25030-164), N2 (Stem Cell Technologies, 07156) and B27 (Life Technologies, 17504044) containing CHIR99021

(3uM, Tocris Bioscience, 4423) and FGF2 (10nM, R&D Systems, 233-FB-001MG/CF) during the assay.

Viability assay

To monitor the viability of WT and EDNRB$^{-/-}$ ENC precursors, cells were assayed for LDH activity using CytoTox 96 cytotoxicity assay kit (Promega, G1780). Briefly, the cells are plated in 96 well plates at 30,000/cm^2. The supernatant and the cell lysate is harvested 24 hours later and assayed for LDH activity using a plate reader (490nm absorbance). Viability is calculated by dividing the LDH signal of the lysate by total LDH signal (from lysate plus supernatant). The cells were cultured in Neurobasal (NB) medium supplemented with L-Glutamine (Gibco, 25030-164), N2 (Stem Cell Technologies, 07156) and B27 (Life Technologies, 17504044) containing CHIR99021 (3μM, Tocris Bioscience, 4423) and FGF2 (10nM, R&D Systems, 233-FB-001MG/CF) during the assay.

High throughput screening

The chemical compound screening was performed using the Prestwick Chemical Library®. The ENC cells were plated in 96 well plates (30,000/cm^2) and scratched manually 24 hours before addition of the compounds. The cells were treated with two concentrations of the compounds (10μM and 1μM). The plates were fixed 24 hours later for total plate imaging. The compounds were scored based on their ability to promote filling of the scratch in 24 hours. The compounds that showed toxic effects (based on dramatic reduction in cell numbers assessed by DAPI staining) were scored 0, compound with no effects were scored 1, compound with moderate effects were scored 2 and compound with strong effects (that resulted in complete filling of the scratch area) were scored 3 and identified as hit compounds. The hits were further validated to ensure reproducibility. The cells were treated with various concentrations of the selected hit compound (Pepstatin A) for dose response analysis. The optimal dose (10μM-based on optimal response and viability) was used for follow-up experiments. For the pre-treatment experiments, cells were CD49D purified at day 11 and treated with Pepstatin A from day 12 through day 15 followed by transplantation into the colon wall of NSG mice. The cells were cultured in Neurobasal (NB) medium supplemented with L-Glutamine (Gibco, 25030-164), N2 (Stem Cell Technologies, 07156) and B27 (Life Technologies, 17504044) containing CHIR99021 (3uM, Tocris Bioscience, 4423) and FGF2 (10nM, R&D Systems, 233-FB-001MG/CF) during the assay.

BACE2 inhibition and Knockdown

To inhibit BACE2, the ENC precursors were treated with 1 μM β-Secretase Inhibitor IV (CAS 797035-11-1 – Calbiochem). To Knockdown BACE2, cells were dissociated using accutase (Innovative Cell Technologies, AT104) and reverse-transfected (using Lipofectamine RNAiMAX-Life Technologies, 13778-150) with a siRNA pool (SMARTpool: ON-TARGETplus BACE2 siRNA, Dharmacon, L-003802-00-0005) or 4 different individual siRNAs (Dharmacon, LQ-003802-00-0002 2 nmol). The Knockdown was confirmed by qRT-PCR measurement of BACE2 mRNA levels in cells transfected with the BACE2 siRNAs vs. the control siRNA pool (ON-TARGETplus Non-targeting Pool, Dharmacon, D-001810-10-05). The transfected cells were scratched 24 hours after plating and fixed 48 hours later for migration quantification. The cells were cultured in Neurobasal

(NB) medium supplemented with L-Glutamine (Gibco, 25030-164), N2 (Stem Cell Technologies, 07156) and B27 (Life Technologies, 17504044) containing CHIR99021 (3uM, Tocris Bioscience, 4423) and FGF2 (10nM, R&D Systems, 233-FB-001MG/CF) during the assay.

Statistical analysis

Data are presented as mean ± SEM and were derived from at least 3 independent experiments. Data on replicates (n) is given in figure legends. Statistical analysis was performed using the Student t-test (comparing 2 groups) or ANOVA with Dunnett test (comparing multiple groups against control). Distribution of the raw data approximated normal distribution (Kolmogorov Smirnov normality test) for data with sufficient number of replicates to test for normality. Survival analysis was performed using log rank (Mantel-Cox) test. Z-scores for primary hits were calculated as $Z= (x-\mu)/\sigma$. X is the migration score value and is 3 for all hit compounds. μ is the mean migration score value and σ is the standard deviation for all compounds and DMSO controls (n=224).

Extended Data

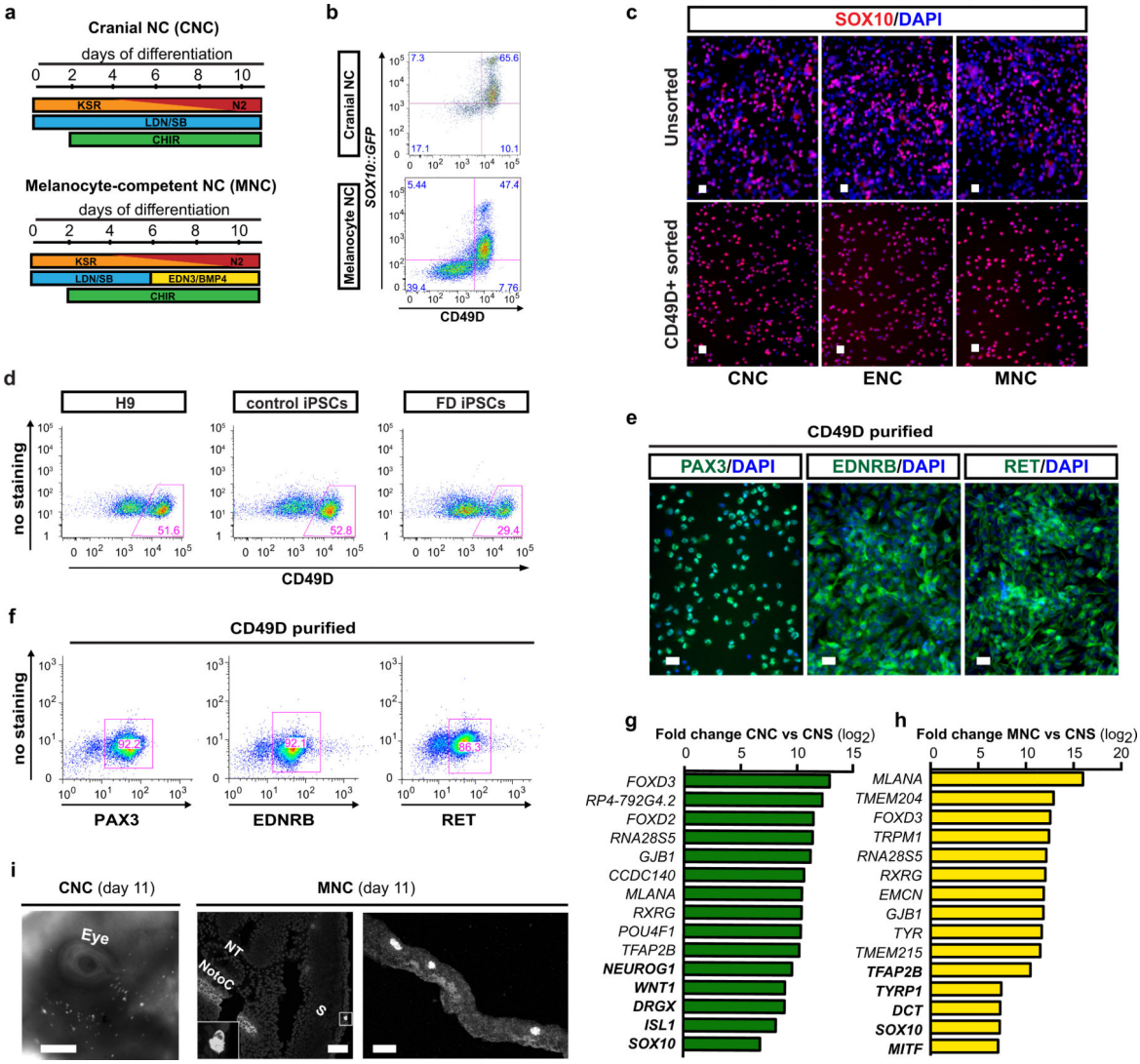

Extended Data Figure 1. Characterization of hESC-derived NC populations

a) Schematic illustration of Cranial NC (CNC) and Melanocyte competent NC (MNC) induction protocols[3]. **b**) Flow cytometry for CD49D and *SOX10::*GFP in CNC and MNC cells. **c**) Immunofluorescence of unsorted and CD49D sorted differentiated NC cells for SOX10. **d)** Flow cytometry for CD49D in ENC derived from H9 hESCs and control and Familial Dysautonomia hiPSCs. **e,f**) Representative immunofluorescence images and flow cytometry in hESC-derived ENC for enteric precursor lineage marker at day 11. **g**) List of the top 10 and selected additional most differentially expressed transcripts from the RNASeq analysis of CNC compared to stage matched CNS precursors[31]. **h**) Lists of the top 10 and selected additional most differentially expressed transcripts from the RNASeq analysis of MNC compared to stage matched CNS precursors[31] **i**) Distribution of CNC and MNC cells in developing chick embryos at 24-36 hours after injection. Right panel: Higher power image of the clusters of MNC cells in the developing surface ectoderm. Abbreviations: NT=

Neural Tube, NotoC= Notochord, S= Somite, Scale bars= 50 μm in c; 25 μm in e; 1 mm in i-left panel; 50 μm in middle and 25 μm in right panel.

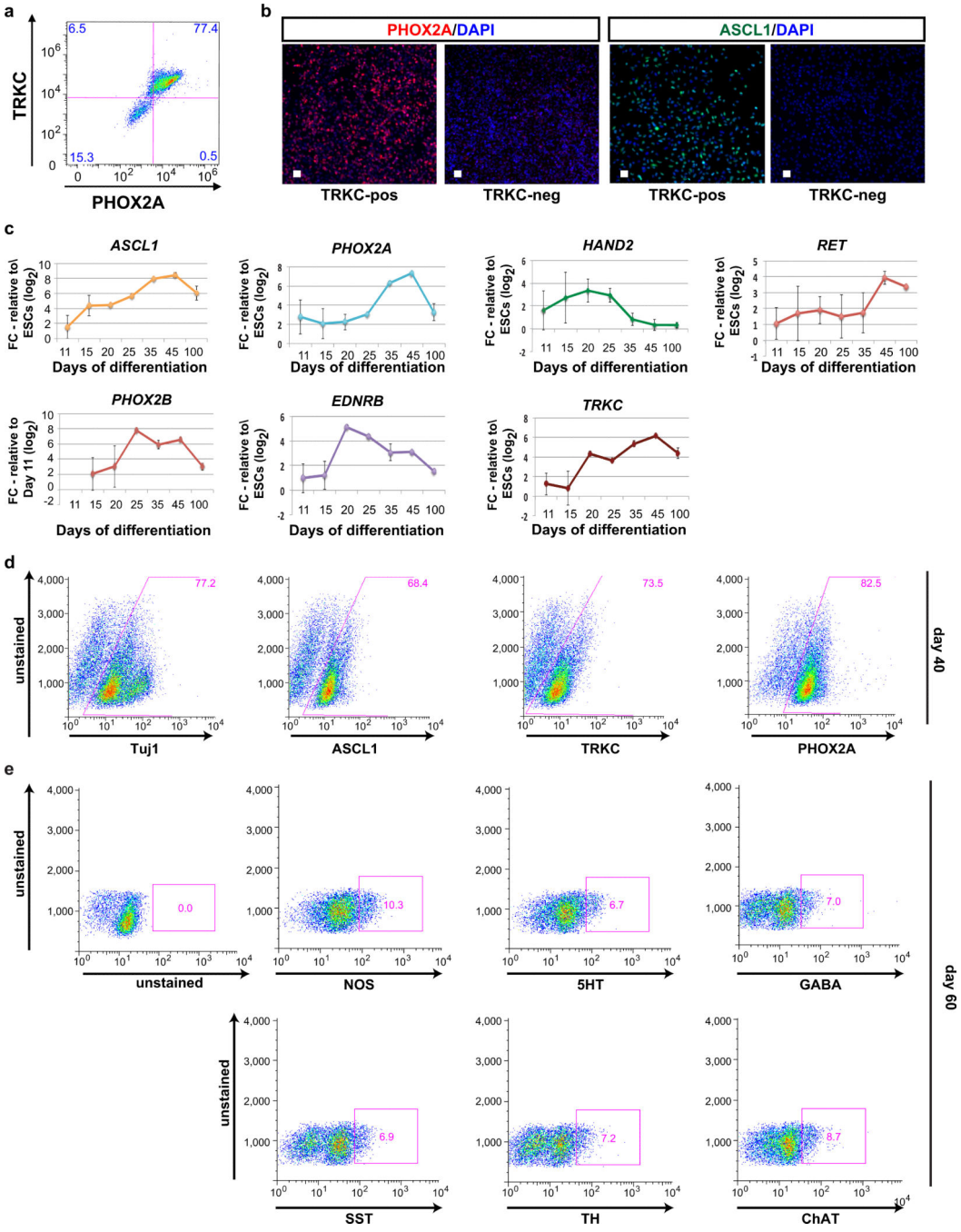

Extended Data Figure 2. Characterization of hESC-derived enteric neural lineages

a) Flow Cytometry for TRKC and PHOX2A expression. **b**) Immunofluorescence for PHOX2A and ASCL1 for TRKC positive and TRKC negative hESC-derived ENC precursors. **c**) Time course qRT-PCR analysis of enteric lineage markers during more extended *in vitro* differentiation periods. n=3 independent experiments. **d,e**) Flow cytometric

quantification of enteric neuron precursor and neuronal markers in ENC-derived neurons at day 40 and 60 of differentiation. n=3 independent experiments. Scale bars= 50 μm; Abbreviation: FC= Fold Change.

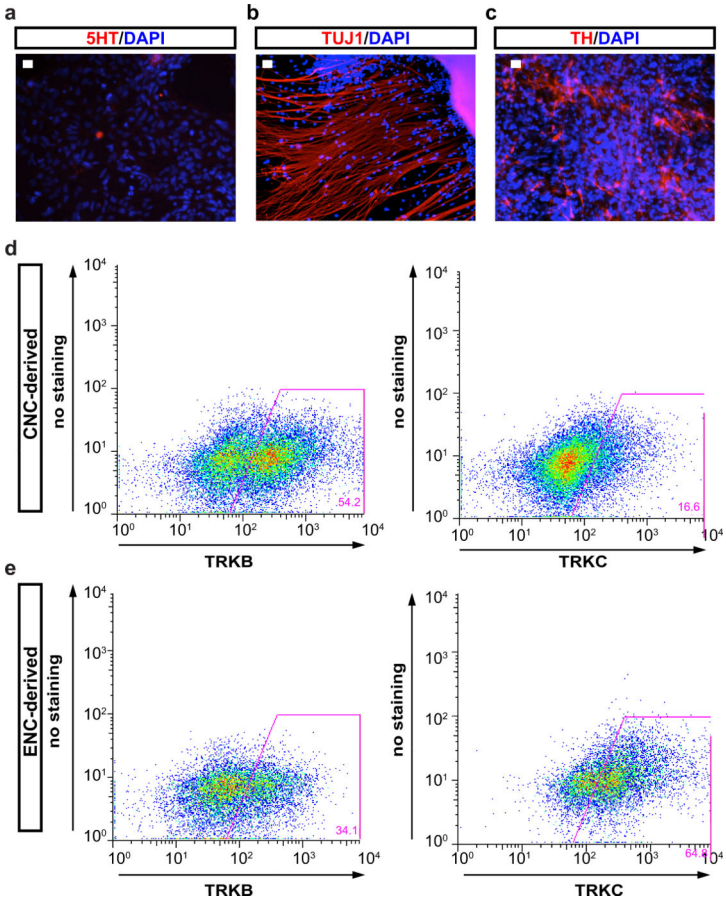

Extended Data Figure 3. CNC gives rise to neurons enriched in autonomic lineage

a-c) Representative immunofluorescence images for expression of 5-HT (Serotonin), TUJ1 and TH in CNC-derived neurons. In contrast to ENC-derived lineages no serotonergic (5HT +) neurons were detected under cranial conditions despite the presence of many Tuj1+ neurons and increased percentages of TH+ cells. **d,e**) Flow Cytometry for TRKB and TRKC under CNC and ENC conditions. n=3 independent experiments. Scale bars= 50 μm.

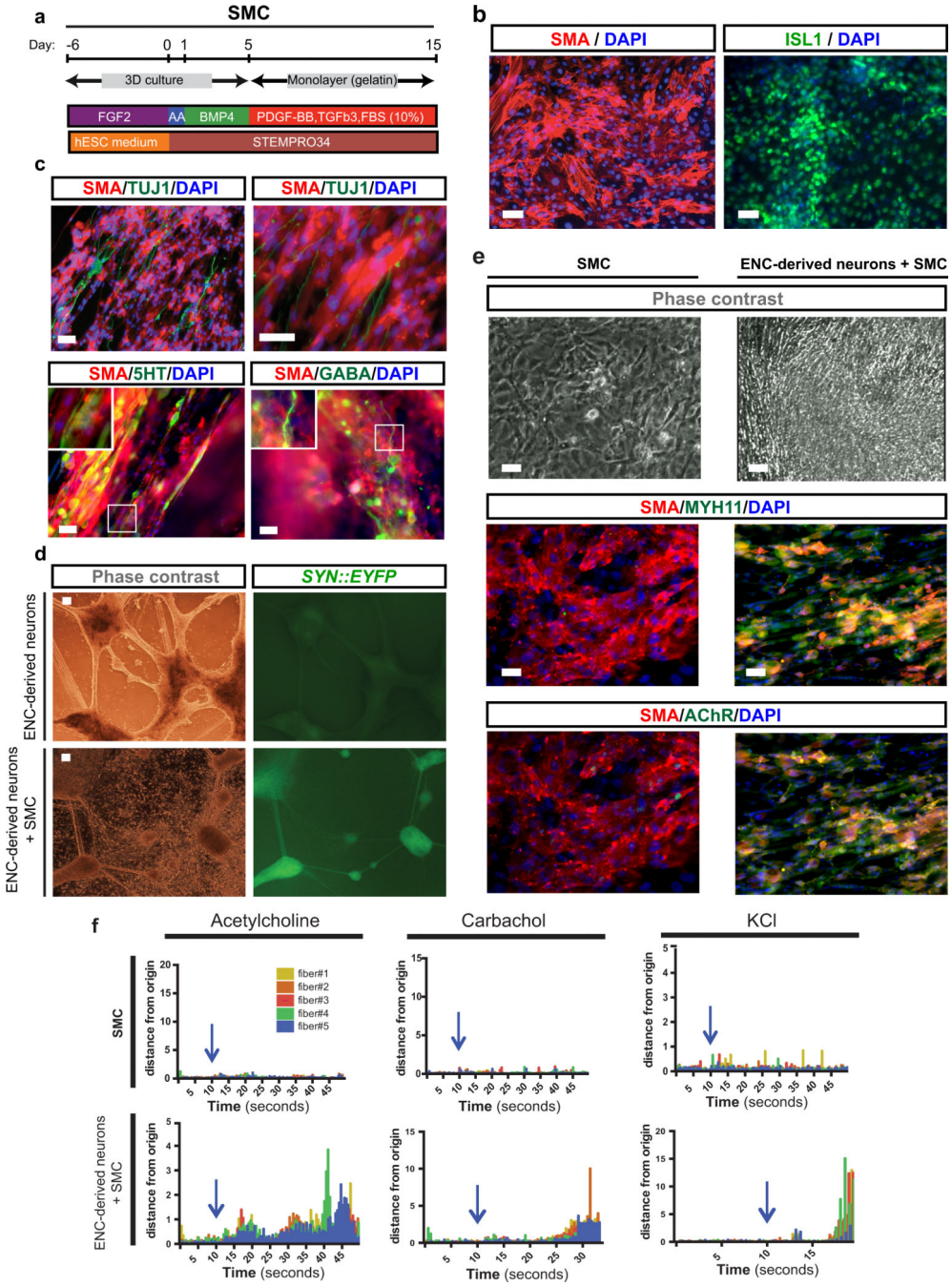

Extended Data Figure 4. Functional characterization of hESC-derived enteric neurons in co-culture with SMCs

a) Schematic illustration of smooth muscle cell (SMC) differentiation protocol. **b**) Immunofluorescence staining of SMC progenitors for SMA and ISL1. **c**) Association of various ENC-derived neuron subtypes with SMA+ cells. **d**) *Synapsin::EYFP* expression in ENC-derived neurons at 40 days of co-culture with SMCs and stage matched neurons in the absence of SMCs. **e**) Monoculture of SMCs versus co-cultures of SMCs with ENC-derived neurons. Upper panels: phase contrast images showing morphological changes of SMCs in Co-culture. Lower panels: Immunofluorescence staining of mature SMC markers MYH11

and Acetylcholine Receptor (AchR) in monoculture of SMCs versus co-cultures of SMCs with ENC-derived neurons. **f**) Diagrams representing extent of contraction of SMC cultures. Arrows indicate the time of pharmacological stimulation. Scale bars= 50 μm in b,c,e; 100 μm in d.

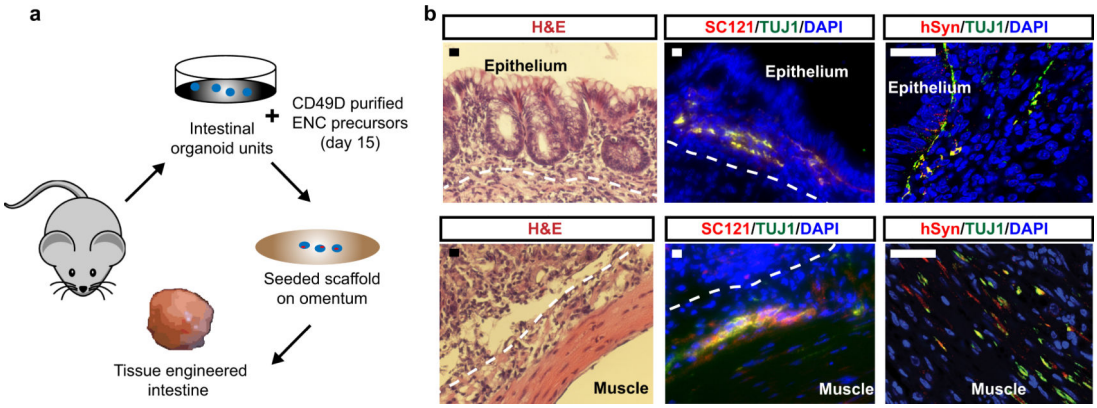

Extended Data Figure 5. Generation of tissue engineered colon using hESC-derived ENC precursors

a) Schematic illustration for generation of tissue engineered colon (TEC). **b**) TEC stained for human cytoplasmic marker SC121 and human specific Synaptophysin (hSYN). Dotted line shows approximate location of border between muscle and epithelial/submucosal-like layers. Scale bars = 20 μm in b-left and middle panels; 40 μm in b-right panel.

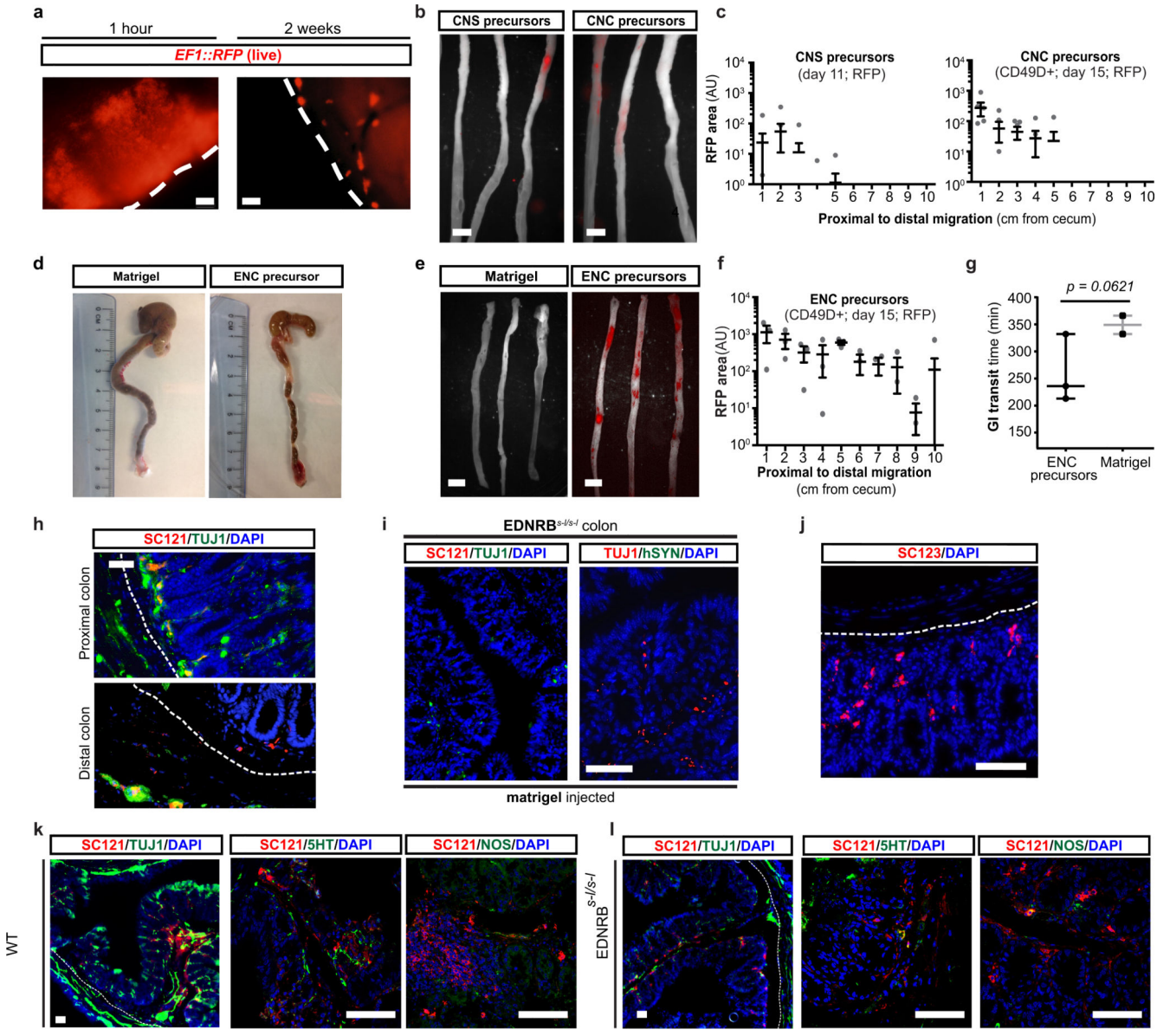

Extended Data Figure 6. Characterization of transplanted hESC-ENC precursors in adult colon of NSG and EDNRB$^{s\text{-}l/s\text{-}l}$ mice

a) Whole mount microscopy of colon transplanted with RFP+ CD49D purified hESC-ENC precursors to track RFP expression at injection site at 1 hour after transplantation to ensure that cells were injected at proper location, and at 2 weeks to show dispersal of the cells and congregation of subset of cells into distinct clusters. The dashed lines indicate the outer border of the intact colon tissue. **b,c**) Whole mount fluorescence imaging and quantification of migration of grafted RFP+ hESC-derived CNS precursors and CD49D purified CNC precursors inside the adult colon wall. **d**) Megacolon-like phenotype in control animals versus animals receiving hESC-derived ENC transplants. **e,f**) Whole mount fluorescence imaging and quantification of migration of grafted RFP+ CD49D purified hESC-ENC precursors in colon of EDNRB$^{s\text{-}l/s\text{-}l}$ mice. **g**) Total GI transit times by carmine dye gavage of EDNRB$^{s\text{-}l/s\text{-}l}$ mice grafted with RFP+ CD49D purified hESC-ENC precursors versus

matrigel only grafted mice. n=3 for grafted animals, n=2 for matrigel group. Note: n=2 for matrigel group was due to the fact that nearly all matrigel injected animals died due to their disease phenotype. **h**) Representative images of grafted hESC-derived enteric NC precursors at 3 months after transplantation into the colon of EDNRB$^{s\text{-}l/s\text{-}l}$ mice co-expressing TUJ1 and SC121. **i**) Immunofluorescence staining of cross sections of HD colons transplanted with matrigel or RFP+ hESC-derived ENC precursors showing expression of SC121 and human specific Synaptophysin (hSYN). **j**) Representative image of grafted hESC-derived enteric NC precursors at 3 months after transplantation into the colon of EDNRB$^{s\text{-}l/s\text{-}l}$ mice expressing human specific GFAP (SC123). **k,l**) Representative images of grafted hESC-derived ENC precursors at 6 weeks after transplantation into the colon of NSG (WT) and EDNRB$^{s\text{-}l/s\text{-}l}$ mice. The dashed lines indicate the border between submucosal and muscle layers. Scale bars= 200 μm in a; 1 cm in b and d; 100 μm in h-l; Abbreviation: AU= Arbitrary Unit. p-value for (**g**) is given numerically, t-test with Welch's correction; n = 3 independent experiments.

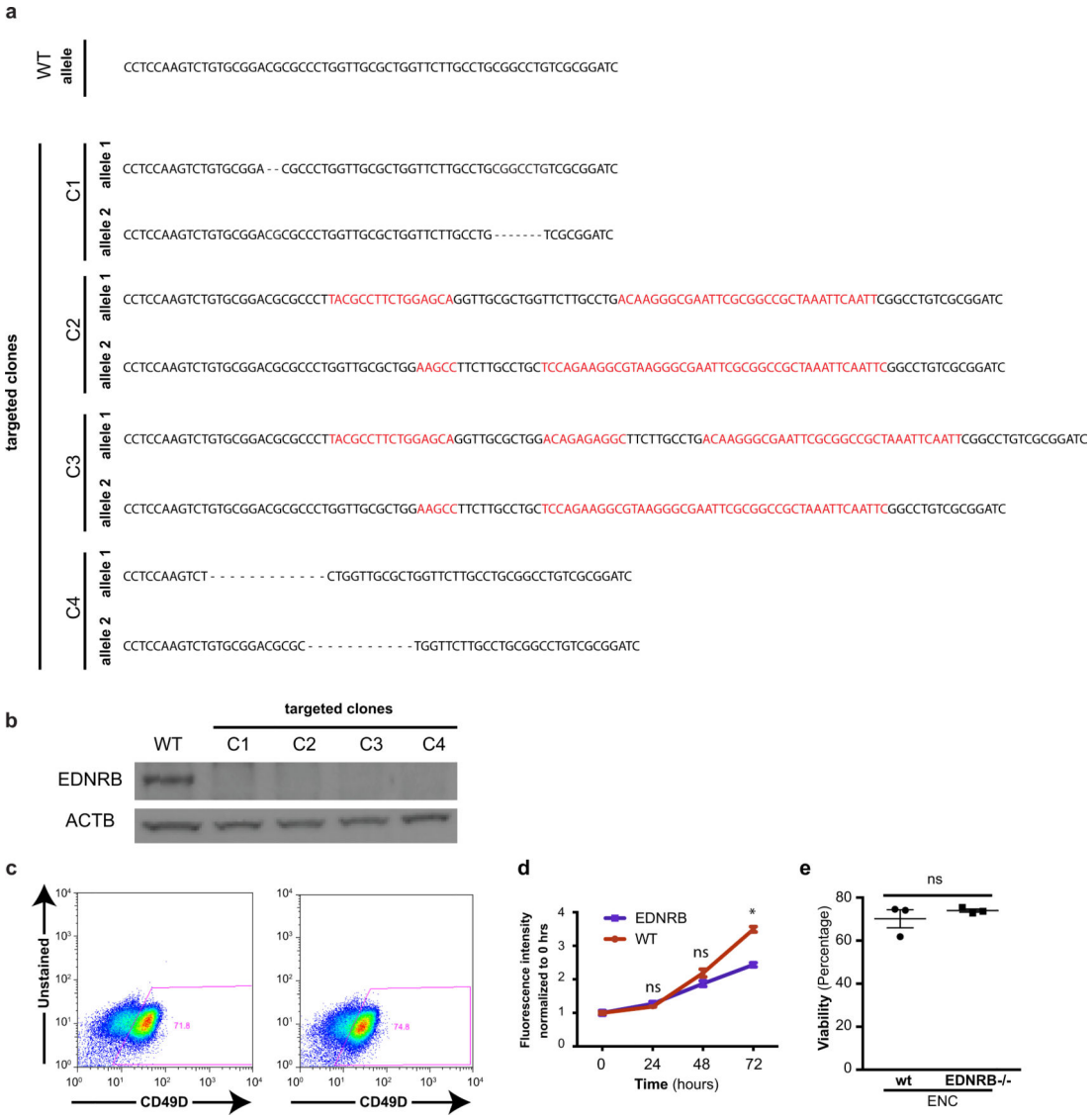

Extended Data Figure 7. Establishing and characterizing EDNRB null hESC lines

a) Sequences of WT and Cas9-nickase induced bi-allelic nonsense mutations in targeted region of EDNRB−/− clones. **b**) Western blot analysis for EDNRB in hESC-derived ENC precursors showing lack of protein expression in mutant clones C1-C4. **c**) EDNRB$^{-/-}$ hESCs can be efficiently differentiated into CD49D+ hESC-derived ENC based on CD49D expression (**c**) and expression of SOX10 (data not shown). **d**) proliferation of EDNRB$^{-/-}$ hESC-derived ENC (day 11) versus WT-derived cells. n = 4 independent experiments. **e**) LDH activity measurement of cell viability in EDNRB$^{-/-}$ hESC-derived ENC (day 11) versus WT-derived cells. p-value in (**d**) is: * $p < 0.05$, t-test, n = 3 independent experiments.

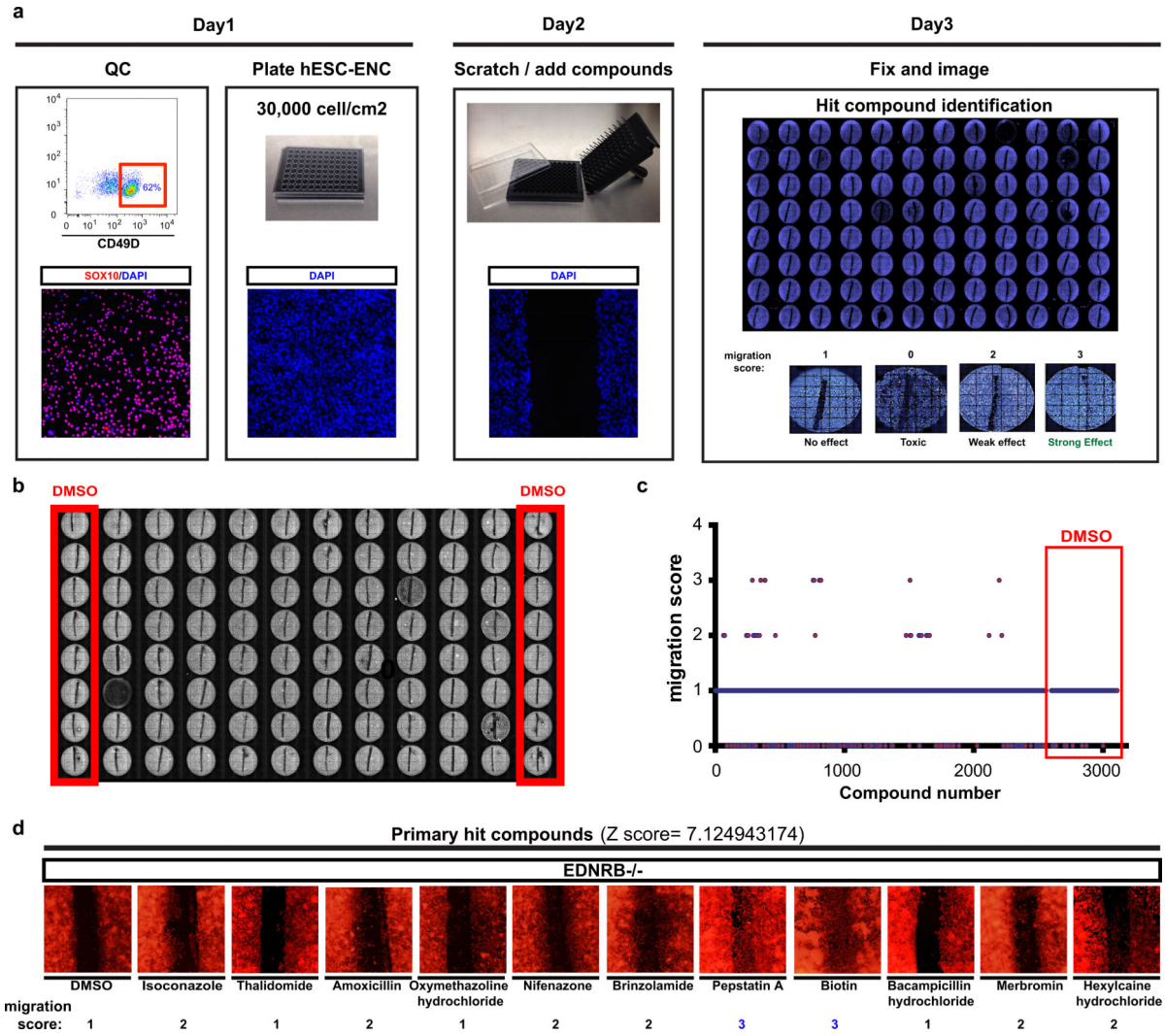

Extended Data Figure 8. Chemical screening for compounds that rescue migration of EDNRB$^{-/-}$ hESC-derived NC precursors

a) Schematic illustration of the time line and experimental steps involved in the chemical screening assay and migration scoring system. **b**) Example of a screening plate layout and locations of DMSO control wells. **c**) Migration scores of Prestwick library compounds and DMSO controls **d**) migration assay and scores for EDNRB$^{-/-}$ hESCs-derived ENC precursors treated with primary hit compounds. Z-score for primary hit compounds in (**c**) is given numerically (compared to DMSO control, n=224 technical replicates)

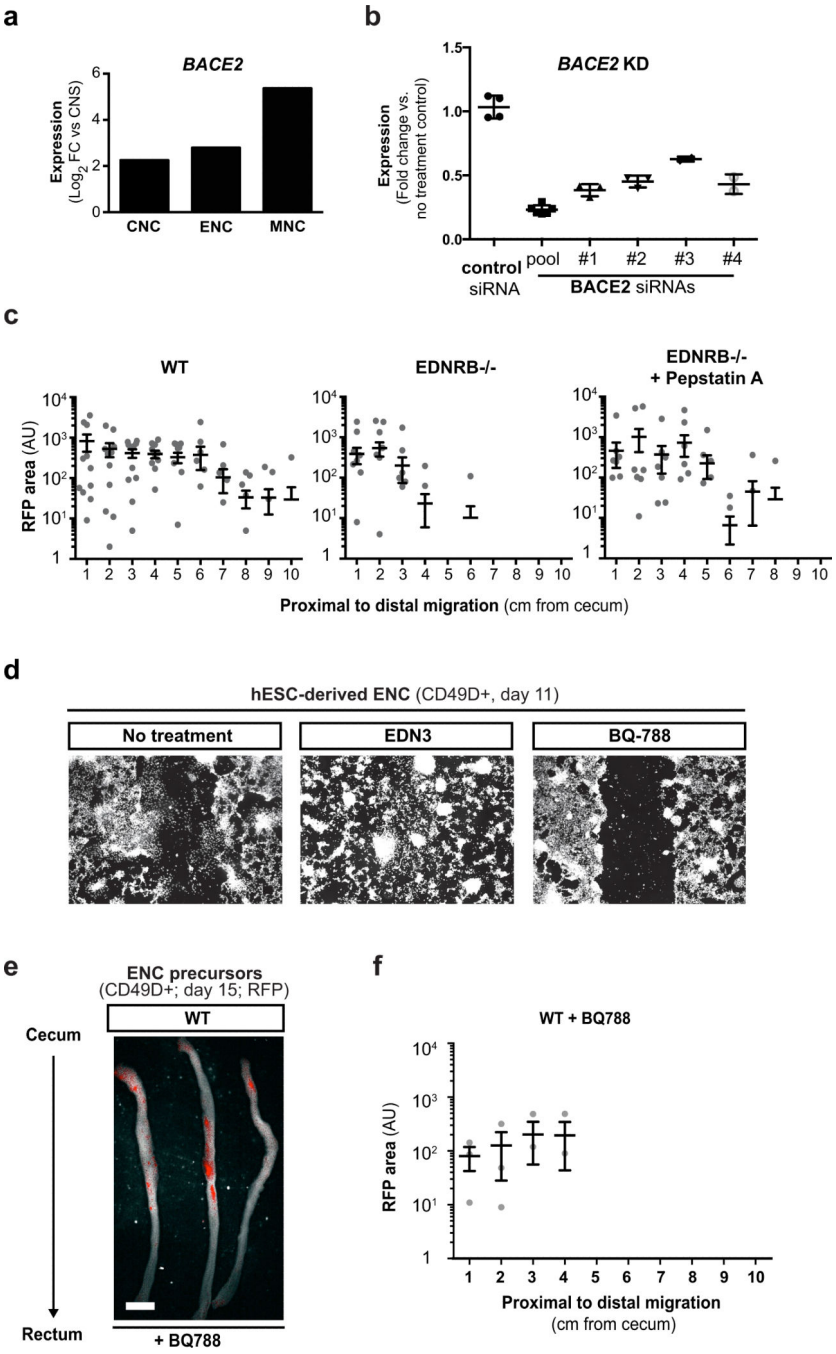

Extended Data Figure 9. Pharmacological modulation of migration in hESC-derived ENC precursors

a) *BACE2* expression in the various hESC-derived NC sublineages at day 11 as compared to stage-matched CNS precursors. **b**) qRT-PCR analysis to confirm knockdown of the *BACE2* in CD49D purified EDNRB–/– hESC-derived ENC after siRNA transfection compared to control siRNA. **c**) Quantification of whole mount images of the colon of NSG mice transplanted with RFP+ CD49D purified WT and EDNRB$^{-/-}$ hESC-derived ENC precursors with or without Pepstatin A pre-treatment (compare to Fig. 4j). **d**) Representative images of

WT CD49D purified hESC-derived ENC treated with EDN3 and BQ-788 (EDNRB inhibitor). **e**) Colon migration assay in WT hESC-derived ENC precursors following pretreatment with BQ788. **f**) Quantification of the data in (**e**). Scale bar = 1 cm in e; Abbreviations: AU= Arbitrary Unit.

Supplementary Material

Refer to Web version on PubMed Central for supplementary material.

ACKNOWLEDGEMENTS

We thank K. Manova (MSKCC molecular cytology core), M. Tomishima (SKI stem cell core) and A. Viale (MSKCC genomics core) for excellent technical assistance and G. Lee (Johns Hopkins University) for hESC-based *PHOX2B::GFP* reporter line. We are very grateful for technical support provided by Harold S. Ralph (Weill Cornell Cell Screening Core), Katherine Brodie (MSKCC Anti-tumor Assessment Core) and the MSKCC Flow Cytometry Core. We would also like to thank J-F Brunet for providing us with the Phox2a antibody and Philip Frykman for kindly sharing their *EDNRB*^{tm1Ywa}/FrykJ HSCR mouse strain. The work was supported by the Starr Foundation and by NYSTEM contract C026446 to L.S.; by grant NS15547 from the NINDS to M.D.G. and by grants RN200946-1 and RN3-06425 from the California Institute for Regenerative Medicine (CIRM) to T.G; by TRI-SCI 2014-030 to L.S., and S.C., and by the New York Stem Cell Foundation (R-103), NIDDK (DP2 DK098093-01) to S.C. S. C is a New York Stem Cell Foundation – Robertson Investigator. J.S. was supported by a DFG fellowship. We would like to thank M. Tomishima, V. Tabar for valuable comments on the manuscript.

REFERENCES

1. Gershon, M. The Second Brain - A Groundbreaking New Understanding of Nervous Disorders of the Stomach and Intestine. Harper Collins; 1999.
2. Heanue TA, Pachnis V. Enteric nervous system development and Hirschsprung's disease: advances in genetic and stem cell studies. Nat Rev Neurosci. 2007; 8:466–479. [PubMed: 17514199]
3. Mica Y, Lee G, Chambers SM, Tomishima MJ, Studer L. Modeling neural crest induction, melanocyte specification, and disease-related pigmentation defects in hESCs and patient-specific iPSCs. Cell Rep. 2013; 3:1140–1152. [PubMed: 23583175]
4. Chan KK, et al. Hoxb3 vagal neural crest-specific enhancer element for controlling enteric nervous system development. Dev Dyn. 2005; 233:473–483. [PubMed: 15768390]
5. Fu M, Lui VC, Sham MH, Cheung AN, Tam PK. HOXB5 expression is spatially and temporarily regulated in human embryonic gut during neural crest cell colonization and differentiation of enteric neuroblasts. Dev Dyn. 2003; 228:1–10. [PubMed: 12950074]
6. Wichterle H, Lieberam I, Porter JA, Jessell TM. Directed differentiation of embryonic stem cells into motor neurons. Cell. 2002; 110:385–397. [PubMed: 12176325]
7. Lee G, et al. Modelling pathogenesis and treatment of familial dysautonomia using patient-specific iPSCs. Nature. 2009; 461:402–406. [PubMed: 19693009]
8. Chalazonitis A, et al. Neurotrophin-3 induces neural crest-derived cells from fetal rat gut to develop in vitro as neurons or glia. J Neurosci. 1994; 14:6571–6584. [PubMed: 7965061]
9. Laflamme MA, et al. Cardiomyocytes derived from human embryonic stem cells in pro-survival factors enhance function of infarcted rat hearts. Nature biotechnology. 2007; 25:1015–1024.
10. Steinbeck JA, et al. Functional Connectivity under Optogenetic Control Allows Modeling of Human Neuromuscular Disease. Cell stem cell. 2015
11. Barthel ER, et al. Tissue engineering of the intestine in a murine model. Journal of visualized experiments : JoVE. 2012:e4279. [PubMed: 23222891]
12. Di Lorenzo C, Solzi GF, Flores AF, Schwankovsky L, Hyman PE. Colonic motility after surgery for Hirschsprung's disease. The American journal of gastroenterology. 2000; 95:1759–1764. [PubMed: 10925981]
13. Hotta R, Natarajan D, Burns AJ, Thapar N. Stem cells for GI motility disorders. Curr Opin Pharmacol. 2011; 11:617–623. [PubMed: 22056114]

14. Schafer KH, Micci MA, Pasricha PJ. Neural stem cell transplantation in the enteric nervous system: roadmaps and roadblocks. Neurogastroenterol Motil. 2009; 21:103–112. [PubMed: 19215588]
15. Hotta R, et al. Transplanted progenitors generate functional enteric neurons in the postnatal colon. J Clin Invest. 2013; 123:1182–1191. [PubMed: 23454768]
16. Gariepy CE, Cass DT, Yanagisawa M. Null mutation of endothelin receptor type B gene in spotting lethal rats causes aganglionic megacolon and white coat color. Proc Natl Acad Sci U S A. 1996; 93:867–872. [PubMed: 8570650]
17. Kruger GM, et al. Temporally distinct requirements for endothelin receptor B in the generation and migration of gut neural crest stem cells. Neuron. 2003; 40:917–929. [PubMed: 14659091]
18. Tam PK, Garcia-Barcelo M. Genetic basis of Hirschsprung's disease. Pediatric surgery international. 2009; 25:543–558. [PubMed: 19521704]
19. Cong L, et al. Multiplex genome engineering using CRISPR/Cas systems. Science. 2013; 339:819–823. [PubMed: 23287718]
20. Chakravarti A. Endothelin receptor-mediated signaling in hirschsprung disease. Hum Mol Genet. 1996; 5:303–307. [PubMed: 8852653]
21. Zhang Y, Kim TH, Niswander L. Phactr4 regulates directional migration of enteric neural crest through PP1, integrin signaling, and cofilin activity. Genes Dev. 2012; 26:69–81. [PubMed: 22215812]
22. Yoshida H, et al. Pepstatin A, an aspartic proteinase inhibitor, suppresses RANKL-induced osteoclast differentiation. J Biochem. 2006; 139:583–590. [PubMed: 16567424]
23. Haas HA. Extending the search for folk personality constructs: the dimensionality of the personality-relevant proverb domain. J Pers Soc Psychol. 2002; 82:594–609. [PubMed: 11999926]
24. Torii T, et al. In vivo knockdown of ErbB3 in mice inhibits Schwann cell precursor migration. Biochem Biophys Res Commun. 2014; 452:782–788. [PubMed: 25204498]
25. Wakatsuki S, Araki T, Sehara-Fujisawa A. Neuregulin-1/glial growth factor stimulates Schwann cell migration by inducing alpha5 beta1 integrin-ErbB2-focal adhesion kinase complex formation. Genes Cells. 2014; 19:66–77. [PubMed: 24256316]
26. Zeltner N, Lafaille FG, Fattahi F, Studer L. Feeder-free derivation of neural crest progenitor cells from human pluripotent stem cells. Journal of visualized experiments : JoVE. 2014
27. Hosoda K, et al. Targeted and natural (piebald-lethal) mutations of endothelin-B receptor gene produce megacolon associated with spotted coat color in mice. Cell. 1994; 79:1267–1276. [PubMed: 8001159]
28. Ran FA, et al. Double nicking by RNA-guided CRISPR Cas9 for enhanced genome editing specificity. Cell. 2013; 154:1380–1389. [PubMed: 23992846]
29. Berthold, M., et al. Data Analysis, Machine Learning and Applications Studies in Classification, Data Analysis, and Knowledge Organization. Preisach, Christine; Burkhardt, Hans; Schmidt-Thieme, Lars; Decker, Reinhold, editors. Vol. 38. Springer; Berlin Heidelberg: 2008. p. 319-326.
30. Dreser N, et al. Grouping of histone deacetylase inhibitors and other toxicants disturbing neural crest migration by transcriptional profiling. Neurotoxicology. 2015; 50:56–70. [PubMed: 26238599]
31. Chambers SM, et al. Highly efficient neural conversion of human ES and iPS cells by dual inhibition of SMAD signaling. Nat Biotechnol. 2009; 27:275–280. [PubMed: 19252484]

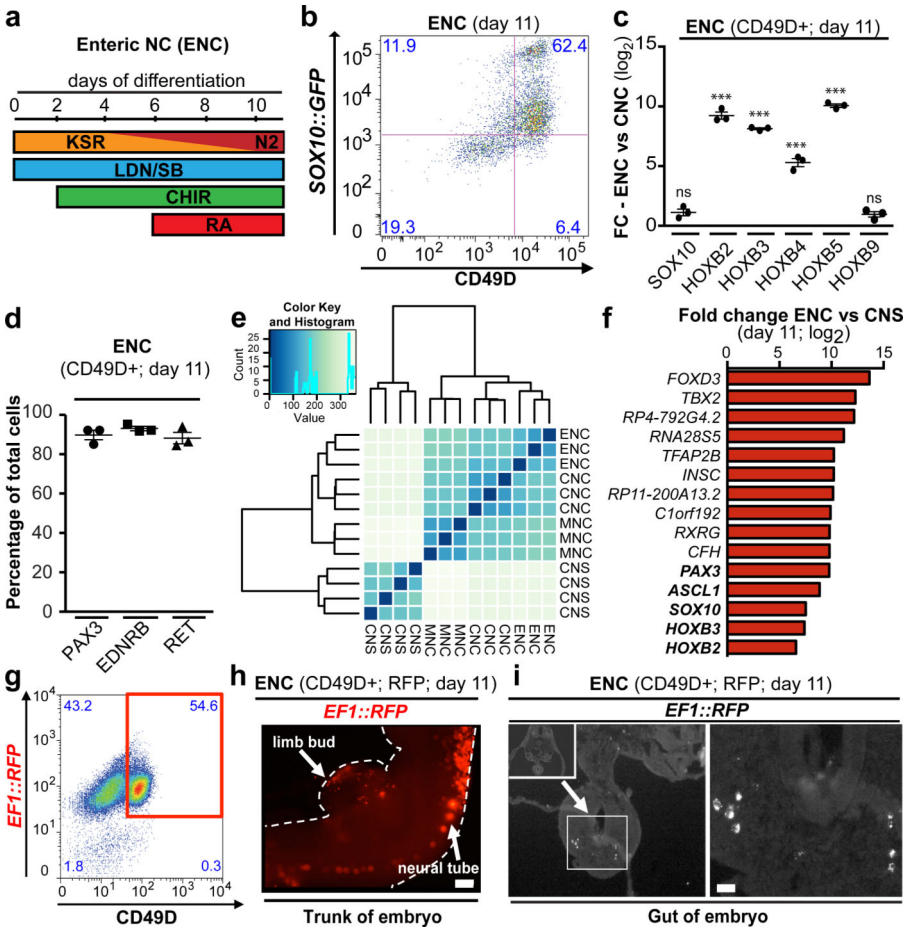

Figure 1. Deriving ENC precursors from hESCs

a) Protocol (day 0-11) for deriving enteric NC (ENC) cells. **b**) Flow cytometry of ENC for *SOX10::GFP* and CD49D at day 11. **c**) qRT-PCR for *SOX10*, vagal NC markers *HOXB2-5* and *HOXB9* in CD49D+ ENC versus CNC, n=3 independent experiments. **d**) Quantification of PAX3, RET and EDNRB immunofluorescence in CD49D+ ENC, n=3 independent experiments. **e**) Unsupervised clustering of CD49D+ NC versus matched CNS precursor (day 11). **f**) Top 10 and selected additional (bold) differentially expressed transcripts in CD49D+ ENC versus CNS precursors. **g**) RFP+ and CD49D+ ENC are FACS purified (day 11) for transplantation into developing chick embryos. **h**) Whole mount epifluorescence showing distribution of RFP+ cells 24 hours after injection. **i**) Cross section of the embryos at trunk levels shows RFP+ cells located in the gut anlage (left panel) and at higher magnification (right panel). Scale bar = 200 μm in i; 10 μm in j; Data are mean ± SEM. p-values are: *** $p < 0.001$ (t-test, ENC compared to CNC; n=3)

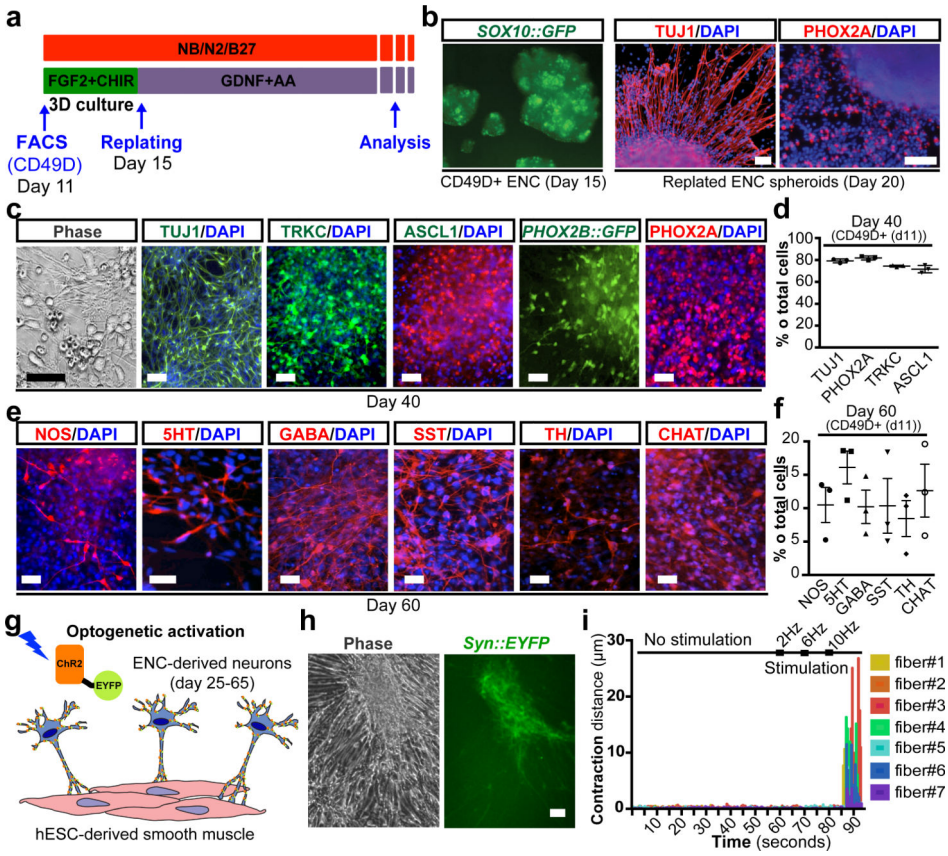

Figure 2. Differentiation of hESC-derived ENC precursors into enteric neuron subtypes

a) Protocol for neuronal differentiation and maturation of ENC precursors **b**) *SOX10::GFP* expressing 3D spheroids from purified ENC gave rise to TUJ1 and PHOX2A enteric neuron lineage. **c-d**) Phase contrast and immunofluorescence images and quantification at day 40. ENC-derived cells express TRKC, ASCL, and PHOX2A/B. PHOX2B expression was confirmed using H9 hESC-based *PHOX2B::GFP* reporter line, n=3 independent experiments. **e-f**) Immunofluorescence analysis and quantification for expression of diverse neurotransmitters. Cells were derived from FACS-purified, CD49D+ ENCs to ensure NC origin, n=3 independent experiments. **g**) Light-stimulated activation of ENC-derived neurons expressing Channelrhodopsin-2 (ChR2). **h**) Phase contrast and live fluorescence images of hESC-derived smooth muscle (SMC) and ENC-derived neuron co-cultures subjected to light stimulation. **i**) Diagrams representing extent of contraction of SMCs before and during light (450nm) stimulation at increasing frequencies. Scale bars = 100 μm in b, (all panels); 50 μm in c, e, h. Data are mean ± SEM.

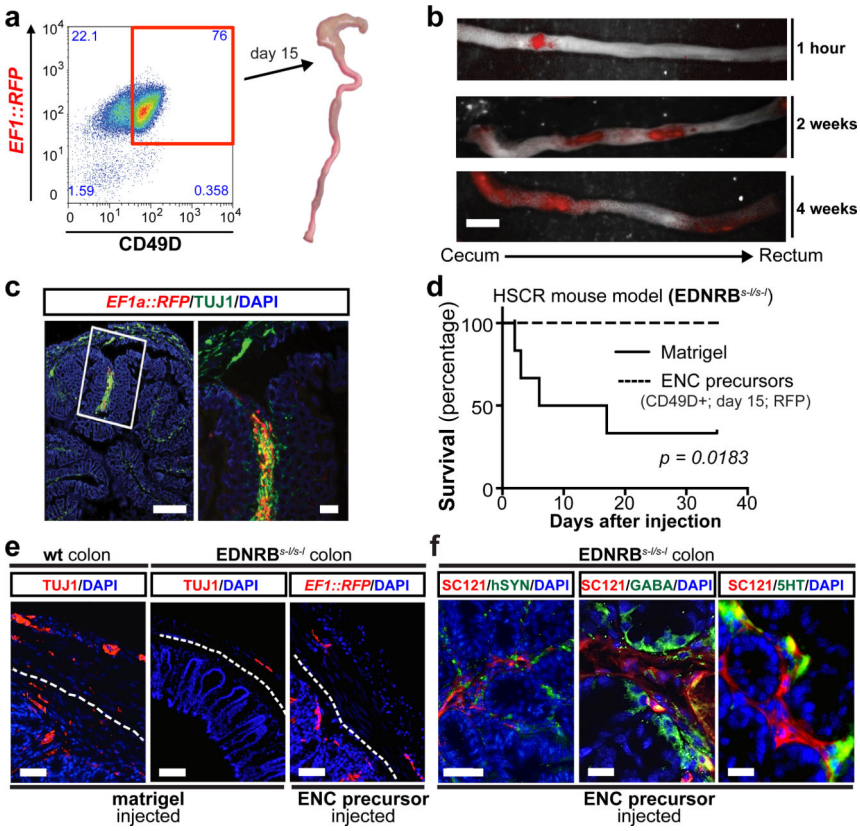

Figure 3. Human ENC precursors migrate extensively in normal and HSCR adult colon

a) Transplantation paradigm into the wall of proximal colon (cecum) of adult mice **b**) Whole mount fluorescence imaging of grafted RFP+ hESC-derived ENC precursors inside adult colon wall (NSG mice). **c**) Cross section of NSG colon showing robust survival and TUJ1 staining of grafted cells. **d**) Survival curve of EDNRB$^{s\text{-}l/s\text{-}l}$ (HSCR) animals grafted with hESC-derived ENC precursors versus matrigel-only. **e**) Immunofluorescence staining of normal or HSCR colons transplanted with matrigel (control) or RFP+ hESC-derived ENC precursors showing distribution of human cells in myenteric and submucosal layers. Dashed lines indicate border between submucosal and muscle layers. **f**) Representative images of grafted animals 3 months after transplantation into EDNRB$^{s\text{-}l/s\text{-}l}$ colon, showing expression of GABA and 5HT in SC-121 human cells. All *in vivo* experiments were performed in a blinded manner. EDNRB$^{s\text{-}l/s\text{-}l}$ mutation was confirmed in all grafted animals, n=6 animals each for treatment and control groups. Scale bars= 1 cm in b; 500 μm in c-left panel; 100 μm in c-right panel, e and 25 μm in f. p-value for survival analysis is given numerically, log-rank (Mantel-Cox) test.

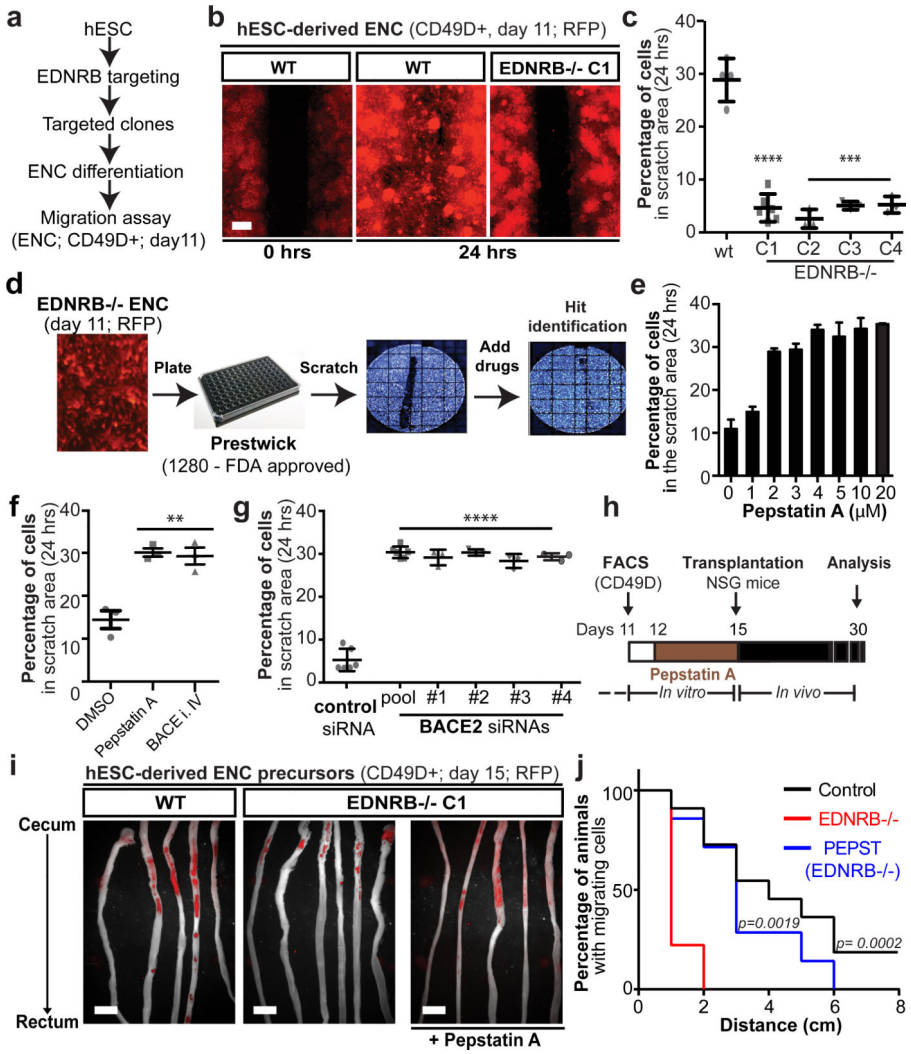

Figure 4. EDNRB signaling regulates human ENC precursor cell migration

a) *In vitro* HSCR disease modeling paradigm. **b-c**) Representative images and quantification of scratch assay in RFP+/CD49D+ WT and EDNRB$^{-/-}$ hESC-derived ENC (clones 1-4), n=3 independent experiments. **d**) Illustration of chemical screen. **e**) Dose-response of Pepstatin A on migration of CD49D+ EDNRB$^{-/-}$ hESC-derived ENC. **f**) Quantification of CD49D+ EDNRB$^{-/-}$ hESC-derived ENC migration following treatment with Pepstatin A (10 μM) or BACE inhibitor IV (1 μM), n=3 independent experiments. **g**) Quantification of cell migration following BACE2 knockdown using pool of 5 different siRNAs or 4 individual siRNAs, n=3 independent experiments. **h)** Pepstatin A pre-transplantation treatment paradigm. **i**) Whole mount images of NSG colon transplanted with RFP+ CD49D purified WT and EDNRB$^{-/-}$ hESC-derived ENC precursors with or without Pepstatin A pre-treatment. **j**) Quantification of the fraction of animals with human cells present in colon at increasing distance from injection site - see **Extended Data Fig. 8C**, n ≥ 8 animals for each of the treatment groups. Scale bars= 200 μm in b; 1 cm in i. Data are mean ± SEM. p-values in **c, f** and h are: ** p<0.01; *** p<0.001; **** p < 0.0001 (ANOVA; Dunnett test

(compared to wt)). p-values for analysis in **l** are given numerically, Log-rank (Mantel-Cox) test; n ≥ 8 per for each group.